Exoplanet Characterisation Observatory (EChO)

Assessment Phase Payload Study

Spectra of low mass stars and planetary objects

ECHO-TN-0001-ENS

Issue 02

Prepared by: France Allard Date: 10-12-2013

Checked / Approved by: Date:

DOCUMENT CHANGE DETAILS

Issue	Date	Page	Description Of Change	Comment

DISTRIBUTION LIST

ECHO Payload Consortium				External	
Co-PIs / Science Team Coordinators		Study Engineering Team Working Group Leads		European Space Agency	
✓	Giovanna Tinetti	✓	Paul Eccleston		Luigi Colangeli
	Hans Ulrik Nørgaard-Nielsen		Ranah Irshad		Kate Isaak
	Jean-Philippe Beaulieu		Emanule Pace		Ludovic Puig
	Paul Hartogh		Gianluca Morgante		Martin Linder
	Giusi Micela		Berend Winter		Roger Walker
	Ignasi Ribas		Marc Ferlet		Matthias Ehle
	Bruce Swinyard		Mercedes Lopez-Morales		Nicola Rando
	Mark Swain		Vince Coudé du Foresto		
	Tanya Lim		Alberto Adriani		
	Neil Bowles		Jean-Michel Reess		
	Enzo Pascale		Marc Ollivier		
	Gillian Wright		Gonzalo Ramos Zapata		
	Graziella Branduardi-Raymont		Neil Bowles		
	Marc Ollivier	**Other Engineering Team**			
	Pierre-Olivier Lagage		*As necessary for doc*		
	Vince Coudé du Foresto				
	Athena Coustenis				
	Emanuele Pace				
	Giuseppe Piccioini				
	Giuseppe Malaguti				
	Alessando Sozzetti				
	Maria Rosa Zapataro Osorio				
	Mercedes Lopez-Morales				
	Enric Palle				
	Christopher Jarchow				
	Denis Grodent				
	Allan Hornstrup				
	Geza Kovacs				
	Pierre Drossart				
	T Encrenaz				
	L Fletcher				
	D Pinfield				
	J Cho				
	F Forget				
	I Waldmann				
	P Deroo				
	I Mueller-Wodarg				
	F Selsis				
	O Grasset				
	L Stixrude				
	T Guillot				
	Others…				

TABLE OF CONTENTS

1 VERY LOW MASS STARS

Very Low Mass stars (VLMs) or stars of less than 0.6 $M_\odot$ (late K to M dwarfs) are the most numerous stars, constituting 90% of the stellar budget and 70% of the total stellar mass of our Galaxy[1,2]. In particular, M dwarfs represent planet host of choice since beyond their predominance, their relatively low mass (0.075 to 0.6 $M_\odot$) and radius (0.1 to 0.7 $R_\odot$) offer ideal conditions for planet detection both by transit spectroscopy and radial velocity. They offer therefore the best characterization possibilities for the lowest mass exoplanets observed with EChO. In preparation of the EChO mission, it will be important to characterize and determine the parameters (mass, radius, T_{eff}, surface gravity, composition: metallicity [M/H], alpha element enhancement [alpha/H], and carbon enrichment [C/O]) of the list of target stars using the most recent VLMs model atmospheres and model interior. In the following we review the current status of model development for these stars.

Since spectroscopic observations of VLMs (late 80s), brown dwarfs and extrasolar planets (mid 90s) are available, one of the most important challenges in modeling their atmospheric, spectroscopic, and evolutive properties lie in high temperature molecular opacities. With the development of computing capacity more reliable and complete list of transitions have been developed over recent years leading to great improvement in the modeling of VLMs. The onset of metal hydride (around T_{eff} ~ 4500 K) and TiO and CO (below T_{eff} ~ 4000 K) absorption band formation occurs in VLMs. Water vapor bands begins to form in early M type dwarfs (below T_{eff} ~ 3900 K). Because oxygen compounds dominate the opacities in the Spectral Energy Distribution (SED) of VLMs, their synthetic spectra and colors respond sensibly to the abundance of oxygen assumed. Allard et al. (2012a,b) and Allard et al. (2013) compared models by different authors and using solar abundance values published over the years and found an improved agreement with constraints for the solar abundances obtained using Radiation HydroDynamic (RHD) simulations by Asplund et al. (2009) and Caffau et al. (2011). In particular, the more conservative values of Caffau et al. (2011) allow perfectly models to match observations of M dwarfs. Higher spectral resolution and up-to-date opacities also contributed to improve VLMs models compared to previous versions. The BT-Settl models reproduce the SED and observed colors across the M dwarfs spectral regime to an unprecedented detail from the optical to the infrared. The *V* band is in particular well reproduced by the new models. In general, the isochrones based on the BT-Settl model atmospheres are in good agreement with the observed colors, even at temperatures below 2800 K. However, some discrepancies remain for some missing molecular absorption bands, in particular in the ultraviolet spectral range. Some discrepancies are also reported for young, low gravity M dwarfs. To address this problem, the implementation of the Mixing Length Theory (MLT) used to treat convection in the BT-Settl models is being revised, and related mixing length is currently being calibrated to the result of RHD simulations by Freytag et al. (2010). Finally, revised VLMs interior models are being developed based on the most up-to-date BT-Settl model atmospheres for 2014.

Below 2800 K, cloud formation is an important factor in the detectability of biosignatures[3], and for the habitability of exoplanets[4]. Hot grains (zirconium oxide, corundum, silicates) cloud formation sets already in the uppermost atmospheric layers of M dwarfs below 2900 K ($T_{gas} \leq 1800$ K), and begin to affect the SED of M dwarfs below $T_{eff} \leq 2500$ K. When grain sizes (or aerosols for planetologists) are large compared to the wavelength, the extinction is dominated by Mie scattering. This is the case for clouds on the Earth, which shine white (Mie scattering is independent on wavelength) with aerosols as large as 300 μm. In VLMs, brown dwarfs and young planet atmospheres, aerosols are smaller (only up to a few μm) which corresponds to the peak wavelength of their SED. This latter is therefore affected mostly by Rayleigh scattering by metals (Fe, Ni, Cu, etc.) in the UV to the near-IR spectral range, and by Mie scattering and absorption by e.g. silicates in the infrared. Grain growth and cloud formation is not a direct observation for these objects. Its effects are only signalled by the gradual depletion of important molecular opacities such as those of TiO, VO, and CaH, the Rayleigh scattering due to submicron-sized dust grains, and by a strong flux redistribution (or greenhouse) effect causing late-type M and L-type brown dwarfs to carry more flux then otherwise predicted at infrared wavelengths[5,6]. The nature of the species that are depleted from the gas phase suggests a silicate grain composition in late M and early L-type brown dwarfs. This conclusion is supported by the detection, in the Spitzer spectrum of an L dwarf, of a shallow absorption feature between 9 and 11 μm attributed to amorphous forsterite[7]. The grains should sink under the influence of gravity (≈ 105 cm^2/s) into deeper layers and vanish from the visible layers of the atmosphere, clearing it from condensable material. Their presence is therefore the sign of important mixing processes in these atmospheres. To account for cloud formation in VLMs, brown dwarfs and extrasolar planets, the BT-Settl models also include therefore a parameter-free cloud model using a mixing defined by the velocity field of radiation hydrodynamic simulations of red and brown dwarfs[8] capable of explaining the change in spectral properties across the M-L-T spectral transition (see Fig. 1). Rajpurohit et al. (2012, 2013) have shown that the BT-Settl model atmosphere grids for VLMs are capable of reproducing the detailed SED of M to L dwarfs. An up to 0.3 mag discrepancy persists however, where models (from all authors) predict too bright J band flux, in the M-L transition between T_{eff} = 2500 and 1800 K. This discrepancy may relate to the treatment of cloud formation in the models. But it is not clear at this point how different cloud models all lead to the same discrepancy, and what error all these cloud model approaches make to

cause similar discrepancy. This is work in progress.

2 BROWN DWARFS AND PLANETARY MASS OBJECTS

Over 1281 brown dwarfs and 32 planetary mass objects detected by imagery are currently known despite their faintness in the solar neighbourhood vicinity. The ever cooler brown dwarfs and free-floating planets that are currently being discovered by the Wide-field Infrared Survey Explorer (WISE)[9,10] and the Canada-France Brown Dwarfs Survey to the Near-Infrared (CFBDSIR)[11], as well as the young gas giant planets discovered by imagery[12], are progressively closing the gap between brown dwarfs and planets. And several infrared integral field spectrographs combined with coronagraph and adaptive optic instruments are coming online (e.g. the Spectro Polarimetric High contrast Exoplanet REsearch or SPHERE at the Very Large Telescope, the Gemini Planet Imager at Gemini south, Project1640 at Mount Palomar, etc.) will further increase the number of characterizable planets. These objects are more directly observable and characterizable than other types of exoplanets which are closer to their parent star. They represent, beyond their own importance, a wonderful test-bench for the understanding of exoplanetary atmospheric properties together with solar system studies in preparation for EChO.

Their atmosphere is, for the young and massive brown dwarfs (1600 K ≤ T_{eff} ≤ 2500 K) similar to those of M dwarf stars in term of their composition and main opacities. Pressure induced H_2 absorption, methane, ammonia and carbon dioxide are detected in late T-type brown dwarfs (300 – 1600 K) which show evidences of a dynamical upwelling of N_2 and CO gas[13–14] seen as an increased of CO band strength, the formation of CO_2 bands and a decrease of NH_3 and CH_4 band absorption. Their cloud composition diversifier with decreasing T_{eff} from zirconium oxide (ZrO_2) and refractory ceramics (perovskite and corundum; $CaTiO_3$, Al_2O_3) in late-M dwarfs, to silicates (enstatite, forsterite, etc.) in early-L dwarfs, and to salts (CsCl, RbCl, NaCl) and ices (H_2O, NH_3, NH_4SH) in late-T and Y dwarfs. This is coherent with the observed weakening and vanishing of TiO and VO molecular bands (via $CaTiO_3$, TiO_2, and VO_2 grains) from the optical spectra of late M and L dwarfs, revealing CrH and FeH bands otherwise hidden by the molecular pseudo-continuum, and the resonance doublets of alkali transitions which are only condensing onto sulfide and chloride salt grains in late-T dwarfs[15]. Grains sizes in their atmosphere range from several microns in the deep clouds to a few nm at high altitudes. Late-type brown dwarfs therefore behave like planets and constitute a fantastic, more easily accessible, laboratory for the study of planetary atmospheres. Besides brown dwarfs may form down to 5 M_{Jup}, i.e. well in overlap with the mass range of planets. It may therefore become difficult if not impossible to tell apart low mass brown dwarfs from exoplanets. It is however possible that the formation mechanisms, and the presence of a core, can be proven for planets if their atmosphere, unlike those of brown dwarfs, carries metal enrichment upwelled by convection from the core. There are questions about if such an upwelling is even possible. But if it is, models are needed to distinguish planets with metal-enrichment by this process from other processes of metal-enrichment (of the interstellar gas from which the planetary system is born). Large grids of models are therefore needed as a function of T_{eff}, log$g$, but also metallicity (scaled to solar, and carbon enrichment).

Fig. 1 shows the important changes in the SED of brown dwarfs across the whole range of effective temperatures and spectral types from VLMs, brown dwarfs and isolated (distant from their host star) exoplanets. The BT-Settl models naturally explain the extreme dusty nature of planetary mass objects found by imagery as an effect of their low gravity. These grids will be extended to a wide range of metallicity in the course of 2014. The BT-Settl models are provided for the entire range of stars below 70,000 K, brown dwarfs and isolated exoplanets observed in the form of synthetic spectra with a high spectral resolution (R=100,000) and theoretical isochrones to the scientific community via the PHOENIX web simulator (http://phoenix.ens-lyon.fr/simulator).

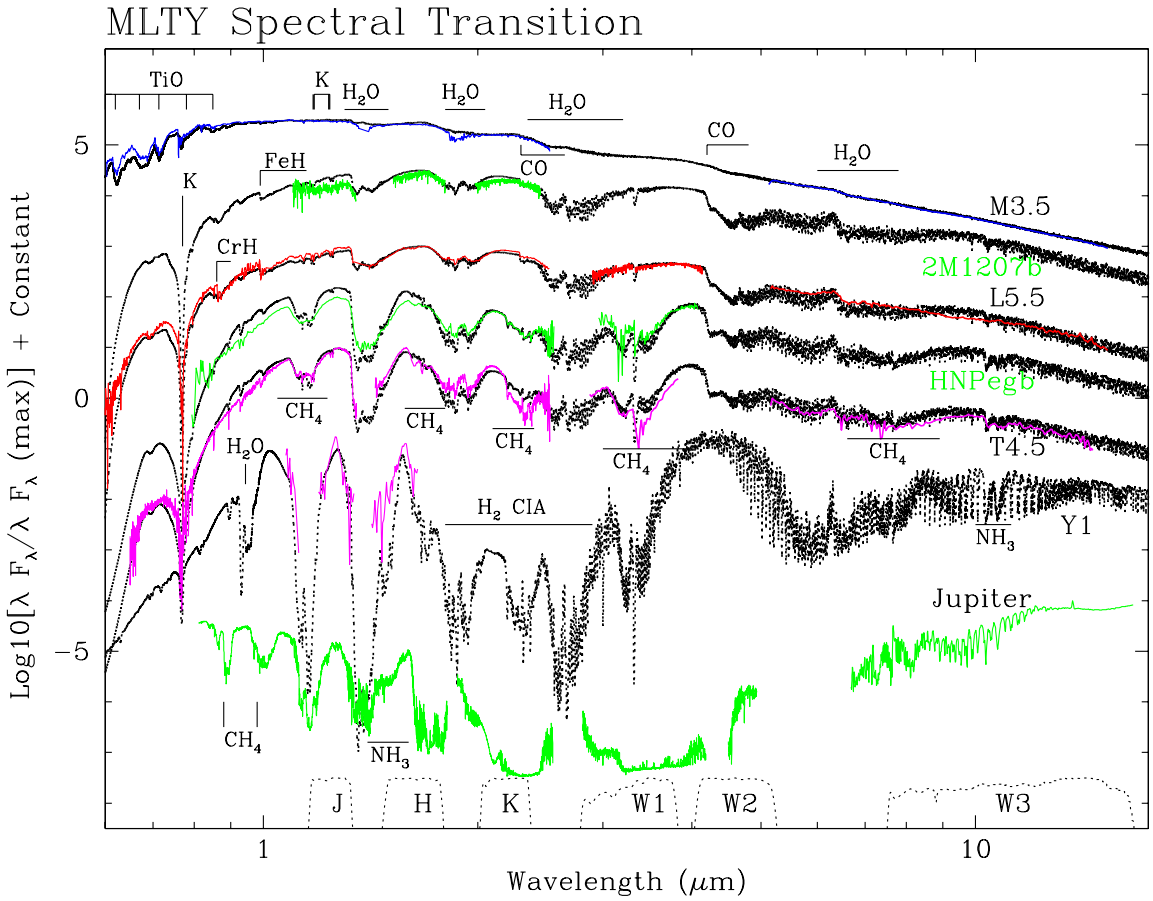

Figure 1. Fig. 1 of Allard et al. (2013). The SED of the M dwarf star Gl 101A (blue curve), the L dwarf 2MASS 1507-16 and the T dwarf 2MASSJ 0559-14 using the United Kingdom Infrared Telescope (UKIRT) and Spitzer (among other) spectroscopic observations[5,6,19], and the Y1 dwarf WISE 0350-5658[20] (magenta curves), as well as those of the planetary mass objects 2M1207b[21], HNPegb[22] and Jupiter (green curves) using the medium-resolution infrared spectrograph SpeX of the NASA InfraRed Telescope Facility (IRTF) on Mauna Kea, SINFONI and Spitzer spectroscopic spectra[23-24], and the infrared spectrum of Jupiter obtained with the Visual and Infrared Mapping Spectrometer (VIMS) onboard Cassini. The BT-Settl models (dotted black curves) are shown for [Teff , logg] = [3000 K, 5.0], [1600 K, 5.0], [1600 K, 5.5], [1200 K, 5.5], [1200 K, 5.5], and [450 K, 5.0] from top to bottom. Also shown are the Mauna Kea Observatories (MKO) and WISE filter bandpasses in the lower part of the diagram (dotted black lines).

REFERENCES:

1. G. Chabrier, *PASP* 115, 763 (2003).

2. G. Chabrier, *The Initial Mass Function 50 Years Later,* E. Corbelli, F. Palla, H. Zinnecker, eds. (2005), vol. 327 of *Astrophysics and Space Science Library,* p. 41.

3. J. F. Kasting, *AGU Fall Meeting Abstracts* p. C1 (2001).

4. T. Tsuji, K. Ohnaka, W. Aoki, *A&A* 305, L1 (1996).

5. S. K. Leggett, P. H. Hauschildt, F. Allard, T. R. Geballe, E. Baron, *MNRAS* 332, 78 (2002).

6. T. R. Geballe, *et al., ApJ* 564, 466 (2002).

7. D. R. Alexander, F. Allard, A. Tamanai, P. H. Hauschildt, *APSS* 251, 171 (1997).

8. Freytag et al. (2010).

9. J. D. Kirkpatrick, *et al., ApJS* 197, 19 (2011).

10. M. C. Cushing, *et al., ApJ* 743, 50 (2011).

11. L. Albert, *et al., AJ* 141, 203 (2011).

12. P. Kalas, *Ipparchos* 2, 23 (2011).

13. C. A. Griffith, R. V. Yelle, *ApJL* 519, L85 (1999).

14. D. Saumon, *et al., ApJ* 647, 552 (2006).

15. Morley et al. (2012).

16. S. K. Leggett, *et al., ApJ* 655, 1079 (2007).

17. J. Paillet, F. Selsis, F. Allard, *Protostars and Planets V* (2005), p. 8341.

18. M. C. Cushing, *et al., ApJ* 648, 614 (2006).

19. M. C. Cushing, *et al., ApJ* 678, 1372 (2008).

20. J. D. Kirkpatrick, *et al., ApJ* 753, 156 (2012).

21. G. Chauvin, *et al., A&A* 438, L25 (2005).

22. K. L. Luhman, *et al., ApJ* 654, 570 (2007).

23. J. Patience, *et al., A&A* 540, A85 (2012).

24. S. K. Leggett, *et al., ApJ* 682, 1256 (2008).